A RAYLEIGH-RITZ ANALYSIS METHODOLOGY

FOR CUTOUTS IN COMPOSITE STRUCTURES[1]

Steven G. Russell
Northrop Corporation
Aircraft Division
Department 3853/82
One Northrop Avenue
Hawthorne, California

ABSTRACT

This paper describes a new Rayleigh-Ritz stress analysis methodology that has been developed for composite panels containing cutouts. The procedure, which makes use of a general assumed displacement field, accommodates circular and elliptical cutouts in biaxially loaded rectangular composite panels. Symmetric integral padups around the cutout can be included in the analysis. Benchmark results are presented to demonstrate the accuracy of the technique, and strength predictions based on the average stress criterion are generated and compared with experimental data. Finally, the stress analysis methodology is integrated into a design procedure for sizing integral padups around circular cutouts, and a sample problem is solved to illustrate its use.

INTRODUCTION

Cutouts of various shapes and sizes occur at numerous locations in typical aircraft structures. These cutouts range in complexity from simple holes designed to accommodate fasteners in bolted wing splices to large, reinforced openings that provide systems routing and access in major fuselage bulkheads. The design of these details in composite structures requires an accurate stress analysis technique and a realistic criterion to predict structural failure.

The analysis of cutouts in orthotropic and anisotropic materials has been the focus of numerous research efforts over the years. Both analytical and numerical methods have been developed for a variety of cutouts under different loading conditions. Many of the analytical methods are based upon the use of complex stress functions from the theory of elasticity. Lekhnitskii (Reference 1) developed analyses for elliptical, triangular, oval, and square cutouts in infinite anisotropic plates under in-plane loading. DeJong (Reference 2) extended this body of work in an analysis of rectangular cutouts with rounded corners in infinite orthotropic plates.

---

[1] This work was performed under NASA/Northrop Contract NAS1-18842, entitled "Innovative Composite Fuselage Structures."

Recently, Prasad and Shuart (Reference 3) developed a general, closed form solution for the moment distribution in infinite anisotropic plates containing circular or elliptical holes and subjected to applied bending moments.

Numerical procedures such as finite element, boundary element, and boundary collocation analysis have been widely used to provide stress analysis of finite plates with cutouts. Hong and Crews (Reference 4) used the finite element method to calculate stress concentration factors around circular holes in uniaxially loaded finite orthotropic plates. The SY5 computer program (Reference 5) uses the finite element method to provide stress analysis for finite isotropic or orthotropic plates with circular, elliptical, square, oval, or rectangular cutouts. Generalized in-plane loading conditions can be accommodated, and padups around cutouts can be modeled using the first three rows of elements around the cutout. The CREPAIR computer program (Reference 6) can be used to analyze elliptical, slotted, and rectangular cutouts in finite orthotropic plates by the boundary element method. CREPAIR is restricted to problems involving biaxial tension/compression or in-plane shear loading conditions. The SASCJ computer code (Reference 7) uses the boundary collocation method to provide stress analysis for loaded fastener holes in finite orthotropic plates. Recently, Klang and Owen (Reference 8) have used the boundary collocation method to develop a stress analysis for finite anisotropic panels containing circular or elliptical cutouts and subjected to in-plane shear loading conditions.

Despite the substantial body of work devoted to stress analysis of orthotropic and anisotropic plates with cutouts, several deficiencies remain in the overall analysis capability. The analytical methods, which are often well-suited for repeated design calculations, are usually valid only for infinite plates. The finite element method requires elaborate preprocessing and postprocessing routines to provide specialized results for cutout problems. The boundary element and boundary collocation approaches, which are especially useful for cutouts with irregular shapes, are difficult to extend to problems involving reinforced cutouts. This paper describes a new approach to cutout stress analysis that is being developed to overcome some of these limitations.

The cutout analysis methodology documented in this paper is based on the Rayleigh-Ritz structural analysis technique, and it makes use of a general assumed displacement field that can be used to treat a wide variety of cutout problems in finite orthotropic plates. This approach eliminates elaborate preprocessing and postprocessing requirements, allows for direct calculation of stress concentration factors at the edge of the cutout, and easily accommodates padups and reinforcements around the hole. As presented here, the methodology is applicable to circular and elliptical cutouts in biaxially loaded orthotropic plates, but it can be extended to include other configurations and loading conditions.

The following sections of the paper provide a description of the Rayleigh-Ritz analysis methodology and a presentation of benchmark results to demonstrate the accuracy of the approach. Next, the analysis methodology is correlated with experimental results and used to generate strength predictions for composite tension specimens with open circular holes. Finally, a design procedure and sample problem are presented to show how the analysis methodology can be used in the design of integral padups around circular cutouts. A complete listing of the equations that are required to implement the cutout analysis methodology is provided in the Appendix.

Consider an elliptical cutout in a biaxially loaded composite panel as shown in **Figure 1**. The panel is modeled as a thin, elastic orthotropic plate under in-plane loading. Due to the symmetry of the cutout geometry and loading, the analysis is confined to the first quadrant x,y > 0 of a rectangular coordinate system with origin at the center of the cutout. Polar coordinates r,θ are defined with respect to the rectangular coordinates x,y by the usual transformation relations r = $(x^2+y^2)^{\frac{1}{2}}$, θ = $\tan^{-1}(y/x)$.

The principle of virtual work for the loaded panel can be expressed as

$$\int_A \delta\{\epsilon\}^T\{N\}dA - \int_S \delta\{u\}^T\{t\}dS = 0 \qquad (1)$$

where,

{u} = vector of panel displacements

{N} = vector of panel stress resultants

{ϵ} = vector of strains at the panel middle surface

{t} = vector of surface tractions applied along the panel boundary

In Equation 1, A is the panel area and S is the curve that defines the panel boundary. The symbol, δ, represents an arbitrary variation of a quantity consistent with the displacement boundary conditions, which require vanishing normal displacements along the axes of symmetry.

Stress analysis of the panel can be carried out using the Rayleigh-Ritz method. In this procedure, an assumed displacement field containing unknown parameters is developed for the panel and substituted into the principle of virtual work, Equation 1, to yield equations for determination of the unknown parameters. The stress analysis of circular or elliptical cutouts in biaxially loaded panels is based upon the assumed displacement field

$$u_r = \sum_{j=0}^{N} \sum_{k=1}^{M} q_j^k f_k(r)\cos 2j\theta$$

$$\qquad (2)$$

$$u_\theta = \sum_{j=0}^{N} \sum_{k=1}^{M} q_j^{M+k} f_k(r)\sin 2j\theta$$

where u_r, u_θ are polar coordinate displacement components and q_j^k are unknown parameters. (NOTE that k is used here as a superscript.) The functions $f_k(r)$ are given by

$$f_k(r) = r^{2(k-M)+1} \quad \text{for } k = 1,\ldots,M \qquad (3)$$

where the superscripted quantity is an exponent. The displacement field of Equation 2 satisfies the symmetry conditions, which require vanishing normal displacement and

shear stress along the x and y axes in **Figure 1**. The parameters M and N in Equation 2 can be adjusted to give the required number of series terms necessary for accurate solution of the problem. Substitution of Equations 2 and 3 into the principle of virtual work leads to a system of linear algebraic equations of the form

$$[K]\{q\} = \{T\} \tag{4}$$

where

$$[K] = \text{stiffness matrix}$$

$$\{q\} = \text{vector of unknown coefficients}$$

$$\{T\} = \text{load vector}$$

Details of the derivation of Equation 4 and the subsequent calculation of panel stresses and strains are given in the Appendix.

The foregoing analysis procedure can be extended to account for the presence of symmetric integral padups around the cutout. Consider an integral padup around a circular cutout as shown in **Figure 2**. The reinforced region, A_1, has thickness t_p and the unreinforced region, A_3, has thickness t. These two constant thickness regions are joined by a tapered region, A_2, where the thickness varies linearly with the radial coordinate. The stiffness matrix [K] for the reinforced panel is calculated by carrying out the integration over the panel area, A, in three parts for regions A_1, A_2, and A_3, respectively. In Region A_2, a linear variation of the extensional stiffness is assumed. Hence,

$$A_{jk}^{(2)} = \frac{(r-R_2)}{(R_1-R_2)} A_{jk}^{(1)} + \frac{(r-R_1)}{(R_2-R_1)} A_{jk}^{(3)} \tag{5}$$

where, R_1, R_2 are defined in **Figure 2**, $A_{jk}^{(i)}$ are the extensional stiffness for region i, and j,k = 1,2, or 6. The general procedure given in the Appendix for calculation of the unreinforced panel stiffness matrix can be used for the reinforced panel as well.

BENCHMARK RESULTS

The analysis methodology discussed in the previous section was implemented in a FORTRAN computer program, and benchmark results were generated to test its accuracy relative to well-established cutout stress analysis techniques. **Figure 3** shows a comparison of results for the stress concentration factor at a circular hole in a uniaxially loaded rectangular plate. Rayleigh-Ritz analysis results were checked against results generated using the anisotropic finite width correction factors developed by Tan (Reference 9). Both (25/50/25) quasi-isotropic (i.e., 25% 0°, 50% ±45°, and 25% 90° plies) and (50/39/11) orthotropic laminates were considered. For both types of laminates, very good agreement was obtained for a wide range of hole diameter/plate width ratios. The Rayleigh-Ritz results shown in **Figure 3** were generated by taking N=5, M=6 in the assumed displacement field given in Equation 2.

Figure 4 shows benchmark results for the stress concentration factor at an elliptical hole in a uniaxially loaded rectangular plate. In this comparison, Rayleigh-Ritz analysis results were again compared with the anisotropic finite width correction factors developed by Tan (Reference 9). The aspect ratio of the ellipse was b/a=2.0, and a (50/39/11) orthotropic laminate was considered. Two different versions of Tan's solution were used. The first version, designated as the basic solution, was developed from an approximate stress analysis for an anisotropic plate containing an elliptical cutout. The second version, designated as the modified solution, was developed to obtain improved agreement between analysis and test data. Figure 4 shows good agreement between the Rayleigh-Ritz solution and Tan's basic solution for cases where $2b/w < 0.5$. For cases where $2b/w \geq 0.5$, the Rayleigh-Ritz solution lies between the two Tan solutions. The Rayleigh-Ritz results shown in Figure 4 were obtained by taking N=15,M=6 in the assumed displacement field given in Equation 2.

Figure 5 shows benchmark results for the stress concentration factor at circular cutouts with symmetric padups in uniaxially loaded rectangular plates. Rayleigh-Ritz analysis results were compared with results for isotropic plates given by Peterson (Reference 10). The Rayleigh-Ritz results were found to agree fairly closely with Peterson's results for padup thicknesses of up to twice the unreinforced panel thickness.

EXPERIMENTAL CORRELATION AND STRENGTH PREDICTION

The strength prediction of composite laminates with cutouts requires that an appropriate stress analysis procedure be combined with a suitable criterion for prediction of material failure. For practical applications, one of the simplest of these material failure criteria is the semi-empirical average stress criterion origi-nally suggested by Whitney and Nuismer (Reference 11). In the average stress crite-rion for uniaxial tension loading, laminate failure is predicted when the average stress over a characteristic material distance, a_0, ahead of the cutout equals the unnotched strength of the laminate. The stress is averaged along the line perpendic-ular to the applied loading that coincides with the symmetry axis of the cutout. The characteristic material distance, a_0, must be determined by correlation with experi-mental data.

To demonstrate the use of the Rayleigh-Ritz cutout stress analysis procedure in an overall strength prediction methodology, the stress analysis was correlated with experimental data to obtain an appropriate value of a_0 for use in the average stress criterion. For this purpose, the strength data published by Tan (Reference 12) for 8-ply AS4/3502 $(0/90/\pm45)_s$ open-hole tension specimens was used. For differ-ent hole sizes, the Rayleigh-Ritz stress analysis procedure was used to calculate laminate stresses in the tension specimens, and the value of a_0 required to bring the average stress criterion prediction into agreement with the experimental failure stress was determined. The a_0 values were generated for circular holes with diame-ters of 0.1, 0.25, 0.3, 0.41, and 0.61 inch. The specimen dimensions given by Tan (Reference 12) for each of these cases were used in the calculations. The average a_0 value for the entire range of hole sizes and specimen dimensions was found to be $a_0 = 0.09$ inch.

To verify the predictive capability of the strength prediction procedure, the ratio of notched to unnotched laminate strength, σ_N/σ_0, was calculated and com-

pared with experimental data published by Nuismer and Whitney (Reference 13). The value $a_o = 0.09$ inch was used in the calculations, which were carried out for 16-ply T300/5208 laminates with $(0/\pm45/90)_{2s}$ and $(0/90)_{4s}$ layups and nominal hole diameters of 0.1, 0.3, 0.6, and 1.0 inch. The specimen dimensions given by Nuismer and Whitney (Reference 13) were used in each of the eight analytical predictions. **Figure 6** shows a comparison between the analytical predictions and experimental data as a function of hole diameter. For the quasi-isotropic $(0/\pm45/90)_{2s}$ laminate, the predictions were 10 to 20 percent conservative for the range of hole sizes considered. The predictions for the orthotropic $(0/90)_{4s}$ laminate were approximately 20 to 30 percent conservative. A plot of predicted versus measured values of σ_N/σ_o for the eight test cases is shown in **Figure 7**.

Based upon the limited number of data considered, the analytical strength prediction procedure for open hole tension specimens seems to provide a conservative estimate of the specimen notched strength. Improved agreement between analysis and experiment can be obtained by adopting a more sophisticated form of the average stress criterion in which the parameter, a_o, is adjusted for different layups and hole sizes. At the time of this writing, experimental correlation and verification of this semi-empirical strength prediction procedure was continuing.

DESIGN PROCEDURE AND SAMPLE PROBLEM

The strength prediction methodology discussed in the previous section can be incorporated into a design procedure for symmetric integral padups around cutouts in composite plates. To illustrate this procedure, consider **Figure 2**, which shows a circular cutout of radius R surrounded by a circular padup in a biaxially loaded composite panel. The padup has a central region of radius R_1 and thickness t_p which tapers to the unreinforced panel thickness t at radius R_2. The object of the design procedure is to determine the padup layup corresponding to a specific uniaxial panel design strength σ_N^*. It is assumed that the padup has the same ply percentages as the parent laminate.

The design task can be carried out by (1) determining the padup region thickness t_p corresponding to σ_N^* and (2) finding a practical padup layup that closely approximates the calculated t_p value. The solution to the first problem can be obtained by iterative application of a strength prediction procedure based on the average stress criterion. For this purpose, consider an unreinforced panel with unit applied load, $N_{x,app}$ (lb/in). The average value of N_x along the x-axis over the line segment $\frac{1}{2}D \leq x \leq \frac{1}{2}D + a_o$ is denoted as $N_{x,av}$. Due to the linear elastic behavior of the panel, the ratio of notched strength, σ_N, to unnotched strength, σ_o, is

$$\frac{\sigma_N}{\sigma_o} = \frac{N_{x,app}}{N_{x,av}} . \tag{6}$$

Next, consider a panel with a padup of the type shown in **Figure 2**. By similar reasoning, the ratio of the notched panel strength, σ_{NP}, for the reinforced panel to the unnotched panel strength is

$$\frac{\sigma_{NP}}{\sigma_o} = \frac{N_{x,app}}{N_{x,av}^*} \frac{t_p}{t} , \tag{7}$$

906

where, $N^*_{x,av}$ is the average stress along the x-axis over the line segment $\frac{1}{2}D \le x \le \frac{1}{2}D+a_0$. The * superscript indicates that the average stress resultant $N^*_{x,av}$ is computed in the reinforced region that has thickness t_p. Since the value of t_p influences the operall load transfer into the padup region from the unreinforced portion of the panel, $N^*_{x,av}$ is a complicated function of t_p.

In the design problem, the desired value of t_p corresponds to the case where $\sigma_{NP} = \sigma^*_N$. For this case, combination of Equations 6 and 7 gives

$$\frac{N^*_{x,av}(t_p)}{N_{x,av}} \frac{\sigma^*_N}{\sigma_N} - \frac{t_p}{t} = 0 \qquad (8)$$

Equation 8 must be solved iteratively to determine the padup region thickness, t_p. For this purpose, a design function, $g(t_p)$, equal to the left-hand side of Equation 8 is introduced. Using two initial estimates for t_p, the secant method can be used to find t_p such that $g(t_p) < \delta$, where δ is a sufficiently small number.

After the padup thickness, t_p, corresponding to σ^*_N has been determined, it remains to find a practical padup layup with the same percentage of plies as the parent laminate. For the case of symmetric integral padups, material of thickness, $(t_p-t)/2$, must be added to each side of the panel. Therefore, the practical padup layup for each side of the panel is the least number of plies that (1) maintains ply percentages of the parent laminate and (2) has total thickness of at least $(t_p-t)/2$.

A flowchart for the padup design procedure is shown in **Figure 8**. To illustrate the use of this procedure, consider a sample problem involving the panel geometry shown in **Figure 2**. The parent laminate is a 36-ply (25/50/25) AS4/3502 panel. The geometrical parameters are L=10 inches, W=4 inches, R=0.5 inch, R_1=0.75 inch, R_2=1 inch, and t=0.1872 inch. The unnotched panel strength is σ_0=71.7 ksi and the panel design strength is σ^*_N=40 ksi. A value a_0=0.09 inch is assumed for the average stress criterion.

For the unreinforced panel with cutout radius R=0.5 inch, the notched panel strength σ_N= 27.1 ksi. Therefore, a padup is necessary if the panel is to withstand the design strength σ^*_N=40 ksi. Using the iterative procedure illustrated in **Figure 8** with initial thickness estimates of t_p=t and t_p=1.1t, the necessary value of t_p was found to be t_p=0.2996 inch. The practical padup corresponding to this value of t_p has 12 plies (three 0°, six ±45°, three 90°) of material on each side of the panel.

For the practical padup, t_p=0.312 inch. A strength analysis for this value of t_p gives a reinforced notched panel strength of σ_{NP}=41.4 ksi. Since this value of σ_{NP} gives a positive margin of safety with respect to the design strength σ^*_N=40 ksi, the padup design procedure has achieved its purpose.

SUMMARY AND FUTURE PLANS

In the previous sections, a Rayleigh-Ritz stress analysis methodology for composite panels with cutouts has been described, and its applications to panel strength prediction and design of symmetric integral padups around cutouts have been illustrated. In its current state of development, this methodology can be applied to

circular or elliptical cutouts in rectangular panels under biaxial tension/ compression loading. The advantages of the procedure are its ability to provide accurate numerical stress analysis solutions with a minimum of input data, and its capability to accommodate cutout reinforcements, such as padups. Its disadvantage is its restricted applicability, which currently includes only a limited number of cutout geometries and panel loading conditions.

Future development efforts for the Rayleigh-Ritz cutout stress analysis methodology will be focused on the incorporation of substructural effects into the analysis, and the extension of the procedure to more complex cutout geometries and loading conditions. The effect of integral stiffeners can be included in the analysis by assuming strain compatibility between the stiffeners and the panel. The strain in the stiffeners can then be calculated using the assumed displacement field given in Equations 2 and 3, and virtual strain energy terms for the stiffener elements can be added to the left-hand side of Equation 1. By this approach, the effect of any number of stiffener elements can be included in the analysis without increasing the number of degrees of freedom in the solution process. An effort to implement the substructural effects analysis for the common case of a "picture-frame" stiffening arrangement around a cutout is currently underway.

Future analysis efforts will also include attempts to extend the existing methodology to include more complex cutout shapes and loading conditions. The analysis of complex cutout shapes, such as slotted holes and rectangles with rounded corners, will require some modification of the basic analysis procedure presented here. One promising approach that will be investigated is use of the penalty function method (Reference 14) in conjunction with the assumed displacement field of Equations 2 and 3. This approach, which involves constructing penalty functions from specified constraint conditions, will make it possible to closely satisfy stress-free boundary conditions along the cutout perimeter without introducing additional degrees of freedom. Further modifications will be required to enable the stress analysis procedure to accommodate more complex loading conditions. For in-plane shear loading, a different assumed displacement field will be constructed to exploit symmetries in the deformation of the panel under this type of loading. This displacement field will be implemented into the analysis using the procedures illustrated in the Appendix. Stress analysis results for problems involving generalized in-plane loading can then be obtained by superposing results obtained from the separate analyses for biaxial and shear loading.

In future work, a concurrent approach to the development of design procedures and enhanced stress analysis methodologies will be pursued. The initial portion of this work, which consists of a design procedure for symmetric integral padups around circular holes in uniaxially loaded panels, was illustrated in this paper. A generalization of this design procedure to permit sizing of cutout reinforcements and stiffening elements will be developed as the extensions to the stress analysis methodology are completed.

REFERENCES

1. Lekhnitskii, S.G., _Anisotropic Plates_, Second Edition, translated from Russian by S.W. Tsai and T. Cheron, Gordon and Breach Science Publishers, 1968.

2. DeJong, Theo, "Stresses Around Rectangular Holes in Orthotropic Plates," _Journal of Composite Materials_, Volume 15, 1981, pp 311-328.

3. Prasad, C.B. and Shuart, M.J., "Moment Distributions Around Holes in Symmetric Composite Laminates Subjected to Bending Moments," _AIAA Journal_, Volume 28, 1990, pp 877-882.

4. Hong, C.S. and Crews, J.H., Jr., "Stress Concentration Factors for Finite Orthotropic Laminates With a Circular Hole and Uniaxial Loading," NASA TP-1469, May 1979.

5. Eisenmann, J.R., "Stress Distribution Around Cutouts," General Dynamics, Convair Aerospace Division, Report FZM-5555, August 1970.

6. Hinkle, T. and Hoehn, G., "Verification of Analytical Methodology for Designing Repairs to Composite Skin, Volume I - Theoretical Development and Test Correlations," McDonnell Aircraft Company, AFWAL-TR-87-3049, Volume I, October 1987.

7. Ramkumar, R.L., Saether, E.S., and Cheng, D., "Design Guide for Bolted Joints in Composite Structures," Northrop Corporation, AFWAL-TR-85-3064, August 1985.

8. Klang, E.C. and Owen, V.L., "Shear Buckling of Specially Orthotropic Plate With Centrally Located Cutouts," Proceedings of the Eighth DoD/NASA/FAA Conference on Fibrous Composites in Structural Design, November 1989.

9. Tan, S.C., "Finite-Width Correction Factors for Anisotropic Plate Containing a Central Opening," _Journal of Composite Materials_, Volume 22, 1988, pp 1080-1097.

10. Peterson, R.E., _Stress Concentration Factors_, John Wiley and Sons, New York, 1974.

11. Whitney, J.M. and Nuismer, R.J., "Stress Fracture Criteria for Laminated Composites Containing Stress Concentrations," _Journal of Composite Materials_, Volume 8, 1974, pp 253-265.

12. Tan, S.C., "Laminated Composites Containing an Elliptical Opening II. Experiment and Model Modification," _Journal of Composite Materials_, Volume 21, 1987, pp 949-968.

13. Nuismer, R.J. and Whitney, J.M., "Uniaxial Failure of Composite Laminates Containing Stress Concentrations," _Fracture Mechanics of Composites_, ASTM STP 593, American Society for Testing and Materials, 1975, pp 117-142.

14. Cook, R.D., _Concepts and Applications of Finite Element Analysis_, Second Edition, John Wiley and Sons, New York, 1981.

For problem solution, it is convenient to represent the assumed panel displacements given in Equation 2 in the matrix form

$$\{u\} = \begin{Bmatrix} u_r \\ u_\theta \end{Bmatrix} = \sum_{j=0}^{N} [U_j]\{q_j\}$$ (A-1)

where $\{q_j\}$ is a vector of dimension 2M containing unknown parameters and $[U_j]$ is a 2 x 2M matrix of the form

$$[U_j] = \begin{bmatrix} f_1\cos2j\theta & \ldots & f_M\cos2j\theta & 0 & \ldots & \ldots & 0 \\ 0 & \ldots & \ldots & 0 & f_1\sin2j\theta & \ldots & f_M\sin2j\theta \end{bmatrix}$$ (A-2)

The strain vector $\{\epsilon\}$ is obtained by applying the strain-displacement relations for polar coordinates:

$$\{\epsilon\} = \begin{Bmatrix} \epsilon_r \\ \epsilon_\theta \\ \gamma_{r\theta} \end{Bmatrix} = \begin{bmatrix} \dfrac{\partial}{\partial r} & 0 \\ \dfrac{1}{r} & \dfrac{1}{r}\dfrac{\partial}{\partial\theta} \\ \dfrac{1}{r}\dfrac{\partial}{\partial\theta} & \dfrac{\partial}{\partial r} - \dfrac{1}{r} \end{bmatrix}\{u\}$$ (A-3)

Substitution of Equations A-1 and A-2 into Equation A-3 leads to a relation of the form

$$\{\epsilon\} = \sum_{j=0}^{N} [H_j]\{q_j\}$$ (A-4)

where $[H_j]$ is a 3 x 2M matrix whose entries are given by

$$H_{j,1m} = \begin{cases} f'_m\cos2j\theta & \text{for} \quad m = 1,\ldots,M \\ 0 & \text{for} \quad m = M+1,\ldots 2M \end{cases}$$ (A-5)

$$H_{j,2m} = \begin{cases} \dfrac{1}{r}f_m\cos2j\theta & \text{for} \quad m = 1,\ldots,M \\ 2j\dfrac{1}{r}f_{m-M}\cos2j\theta & \text{for} \quad m = M+1,\ldots 2M \end{cases}$$ (A-6)

$$H_{j,3m} = \begin{cases} -2j\dfrac{1}{r}f_m\sin2j\theta & \text{for} \quad m = 1,\ldots,M \\ (f'_m - \dfrac{1}{r}f_m)\sin2j\theta & \text{for} \quad m = M+1,\ldots 2M \end{cases}$$ (A-7)

The superposed prime denotes differentiation with respect to r. The stress resultant vector $\{N\}$ is obtained by application of the stress-strain relations. Let E_x, E_y, G_{xy}, ν_{xy} be the orthotropic elastic constants for the panel. Let

$$\bar{A}_{11} = \frac{E_x t}{1-\nu_{xy}\nu_{yx}} \qquad \bar{A}_{12} = \frac{\nu_{xy}E_y t}{1-\nu_{xy}\nu_{yx}}$$

$$\tag{A-8}$$

$$\bar{A}_{22} = \frac{E_y t}{1-\nu_{xy}\nu_{yx}} \qquad \bar{A}_{66} = G_{xy}t$$

where $\nu_{yx} = \nu_{xy}(E_y/E_x)$ and t is the panel thickness. The stress resultant vector is given by

$$\{N\} = \begin{Bmatrix} N_r \\ N_\theta \\ N_{r\theta} \end{Bmatrix} = \begin{bmatrix} A_{11} & A_{12} & A_{16} \\ A_{12} & A_{22} & A_{26} \\ A_{16} & A_{26} & A_{66} \end{bmatrix} \begin{Bmatrix} \epsilon_r \\ \epsilon_\theta \\ \gamma_{r\theta} \end{Bmatrix}$$

$$\tag{A-9}$$

where

$$A_{11} = \bar{A}_{11}\cos^4\theta + 2(\bar{A}_{12} + 2\bar{A}_{66})\sin^2\theta\cos^2\theta + \bar{A}_{22}\sin^4\theta$$

$$A_{12} = (\bar{A}_{11} + \bar{A}_{22} - 4\bar{A}_{66})\sin^2\theta\cos^2\theta + \bar{A}_{12}(\cos^4\theta + \sin^4\theta)$$

$$A_{16} = -(\bar{A}_{11} - \bar{A}_{12} - 2\bar{A}_{66})\sin\theta\cos^3\theta - (\bar{A}_{12} - \bar{A}_{22} + 2\bar{A}_{66})\sin^3\theta\cos\theta$$

$$A_{22} = \bar{A}_{11}\sin^4\theta + 2(\bar{A}_{12} + 2\bar{A}_{66})\sin^2\theta\cos^2\theta + \bar{A}_{22}\cos^4\theta$$

$$\tag{A-10}$$

$$A_{26} = -(\bar{A}_{11} - \bar{A}_{12} - 2\bar{A}_{66})\sin^3\theta\cos\theta - (\bar{A}_{12} - \bar{A}_{22} + 2\bar{A}_{66})\sin\theta\cos^3\theta$$

$$A_{66} = (\bar{A}_{11} + \bar{A}_{22} - 2\bar{A}_{12} - 2\bar{A}_{66})\sin^2\theta\cos^2\theta + \bar{A}_{66}(\sin^4\theta + \cos^4\theta)$$

Equation A-9 can be written in the compact matrix form

$$\{N\} = [A]\{\epsilon\}$$

$$\tag{A-11}$$

where [A] is the 3 x 3 matrix in Equation A-9.

For the rectangular panel of length L and width W shown in **Figure 1**, the r coordinate defining the boundary is a function of θ given by

$$R_b(\theta) = \begin{cases} \dfrac{L}{2\cos\theta} & \text{for } 0 \leq \theta \leq \phi \\[2ex] \dfrac{W}{2\sin\theta} & \text{for } \phi \leq \theta \leq \dfrac{\pi}{2} \end{cases}$$

$$\tag{A-12}$$

where $\phi = \tan^{-1}(W/L)$. The r coordinate defining the edge of the elliptical cutout is also a function of θ given by

$$R_c(\theta) = \frac{ab}{(a^2\sin^2\theta + b^2\cos^2\theta)^{\frac{1}{2}}}$$

$$\tag{A-13}$$

911

where a,b are the dimensions of the ellipse semiaxes. The surface traction vector along the panel boundary is

$$\{t\} \;=\; \left\{ \begin{array}{c} t_r \\[4pt] t_\theta \end{array} \right\} \tag{A-14}$$

$$t_r \;=\; \left\{ \begin{array}{ll} \dfrac{1}{2}\,N_x(1+\cos2\theta) & \text{for } 0 \le \theta \le \phi \\[10pt] \dfrac{1}{2}\,N_y(1-\cos2\theta) & \text{for } \phi \le \theta \le \dfrac{\pi}{2} \end{array} \right. \tag{A-15}$$

$$t_\theta \;=\; \left\{ \begin{array}{ll} -\dfrac{1}{2}\,N_x\sin2\theta & \text{for } 0 \le \theta \le \phi \\[10pt] \dfrac{1}{2}\,N_y\sin2\theta & \text{for } \phi \le \theta \le \dfrac{\pi}{2} \end{array} \right. \tag{A-16}$$

Introducing Equations A-1, A-4, A-11, and A-14 into Equation 1 leads to a matrix equation of the form

$$[K]\{q\} \;=\; \{T\} , \tag{A-17}$$

where [K] is an M(2N+1) x M(2N+1) stiffness matrix, {q} is an M(2N+1) x 1 vector of unknown displacement field parameters and {T} is an M(2N+1) x 1 load vector.

The stiffness matrix [K] can be represented in the partitioned form

$$[K] \;=\; \begin{bmatrix} [K_{00}] & [K_{01}] & \cdots & & \cdots & [K_{0N}] \\ [K_{10}] & [K_{11}] & \cdots & & \cdots & [K_{1N}] \\ \vdots & \vdots & & & & \vdots \\ \vdots & \vdots & & & & \vdots \\ \vdots & \vdots & & & & \vdots \\ [K_{N0}] & [K_{N1}] & \cdots & & \cdots & [K_{NN}] \end{bmatrix} \tag{A-18}$$

where the partition [K_{00}] is an M x M matrix, the partitions [K_{01}],..., [K_{0N}] are M x 2M matrices, the partitions [K_{10}],...,[K_{N0}] are 2M x M matrices, and the remaining partitions are 2M x 2M matrices. The elements of a general partition [K_{jk}] are given by the relations

$$K_{jk,mn} \;=\; \int_0^{\frac{\pi}{2}} \{[A_{11}\beta_{mn} + A_{12}(\delta_{mn} + \delta_{nm}) + A_{22}\phi_{mn}]\cos2j\theta\cos2k\theta$$

$$- 2k(A_{16}\delta_{nm} + A_{26}\phi_{mn})\cos2j\theta\sin2k\theta$$

$$- 2j(A_{16}\delta_{mn} + A_{26}\phi_{mn})\sin2j\theta\cos2k\theta$$

$$+ 4jkA_{66}\phi_{mn}\sin2j\theta\sin2k\theta\}d\theta$$
$$\tag{A-19}$$

$$\text{for } 1 \le m \le M, \; 1 \le n \le M$$

912

$$K_{jk,mn} = \int_0^{\frac{\pi}{2}} [2k(A_{12}\delta_{n-M,m} + A_{22}\phi_{m,n-M})\cos2j\theta\cos2k\theta$$

$$+ (A_{16}\lambda_{m,n-M} + A_{26}\eta_{m,n-M})\cos2j\theta\sin2k\theta$$

$$- 4jkA_{26}\phi_{m,n-M}\sin2j\theta\cos2k\theta$$

$$- 2jA_{66}\eta_{m,n-M}\sin2j\theta\sin2k\theta]d\theta$$

$$\text{for } 1 \le m \le M, \ M+1 \le n \le 2M \qquad (A-20)$$

$$K_{jk,mn} = \int_0^{\frac{\pi}{2}} [2j(A_{12}\delta_{m-M,n} + A_{22}\phi_{m-M,n})\cos2j\theta\cos2k\theta$$

$$- 4jkA_{26}\phi_{m-M,n}\cos2j\theta\sin2k\theta$$

$$+ (A_{16}\lambda_{n,m-M} + A_{26}\eta_{n,m-M})\sin2j\theta\cos2k\theta$$

$$- 2kA_{66}\eta_{n,m-M}\sin2j\theta\sin2k\theta]d\theta$$

$$\text{for } M+1 \le m \le 2M, \ 1 \le n \le M \qquad (A-21)$$

$$K_{jk,mn} = \int_0^{\frac{\pi}{2}} [4jkA_{22}\phi_{m-M,n-M}\cos2j\theta\cos2k\theta$$

$$+ 2jA_{26}\eta_{m-M,n-M}\cos2j\theta\sin2k\theta$$

$$+ 2kA_{26}\eta_{n-M,m-M}\sin2j\theta\cos2k\theta$$

$$+ A_{66}\omega_{m-M,n-M}\sin2j\theta\sin2k\theta]d\theta$$

$$\text{for } M+1 \le m \le 2M, \ M+1 \le n \le 2M \qquad (A-22)$$

where,

$$\beta_{mn} = \int_{R_c}^{R_b} f_m' f_n' r \, dr \qquad (A-23)$$

$$\delta_{mn} = \int_{R_c}^{R_b} f_m f_n' \, dr \qquad (A-24)$$

$$\phi_{mn} = \int_{R_c}^{R_b} \frac{1}{r} f_m f_n \, dr \qquad (A-25)$$

$$\lambda_{mn} = \int_{R_c}^{R_b} f_m'(f_n' - \frac{1}{r}f_n) r \, dr = \beta_{mn} - \delta_{nm} \qquad (A-26)$$

913

$$\eta_{mn} = \int_{R_c}^{R_b} f_m(f_n' - \frac{1}{r}f_n)dr = \delta_{mn} - \phi_{mn} \tag{A-27}$$

$$\omega_{mn} = \int_{R_c}^{R_b} (f_m' - \frac{1}{r}f_m)dr = \beta_{mn} - \delta_{mn} - \delta_{nm} + \phi_{mn} \tag{A-28}$$

for $1 \le m,n \le M$. In Equations A-23 through A-31, the prime denotes differentiation with respect to r. Using the functions defined in Equation 3, the integrals in Equations A-23 through A-25 can be evaluated to obtain

$$\beta_{mn} = \begin{cases} \dfrac{[2(m-M)+1][2(n-M)+1]}{[2(m+n) - 4M+2]} \left\{ R_b^{[2(m+n)-4M+2]} - R_c^{[2(m+n)-4M+2]} \right\} \\ \qquad\qquad\qquad \text{for } m+n \ne 2M-1 , \\[1em] [2(m-M)+1][2(n-M)+1]\, \ln(R_b/R_c) \\ \qquad\qquad\qquad \text{for } m+n = 2M-1 \end{cases} \tag{A-29}$$

$$\delta_{mn} = \begin{cases} \dfrac{[2(n-M)+1]}{[2(m+n) - 4M+2]} \left\{ R_b^{[2(m+n)-4M+2]} - R_c^{[2(m+n)-4M+2]} \right\} \\ \qquad\qquad\qquad \text{for } m+n \ne 2M-1 , \\[1em] [2(n-M)+1]\ln(R_b/R_c) \\ \qquad\qquad\qquad \text{for } m+n = 2M-1 \end{cases} \tag{A-30}$$

$$\phi_{mn} = \begin{cases} \dfrac{1}{[2(m+n) - 4M+2]} \left\{ R_b^{[2(m+n)-4M+2]} - R_c^{[2(m+n)-4M+2]} \right\} \\ \qquad\qquad\qquad \text{for } m+n \ne 2M-1 , \\[1em] \ln(R_b/R_c) \\ \qquad\qquad\qquad \text{for } m+n = 2M-1 \end{cases} \tag{A-31}$$

The quantities R_b and R_c are functions of θ as defined in Equations A-12 and A-13. The integrals in Equations A-19 through A-22 can be evaluated numerically using Simpson's rule.

The load vector {T} in Equation A-17 can be represented in the partitioned form

$$\{T\} \;=\; \left\{ \begin{array}{c} \{T_0\} \\ \{T_1\} \\ \vdots \\ \{T_j\} \\ \vdots \\ \{T_N\} \end{array} \right\} \qquad\qquad (A\text{-}32)$$

where $\{T_0\}$ is an M x 1 vector and the remaining partitions are 2M x 1 vectors. The elements of a general partition $\{T_j\}$ are given by the relations

$$T_{j,m} \;=\; \frac{1}{2} N_x L \int_0^\phi f_m(R_b)\cos 2j\theta\, d\theta$$

$$\qquad +\; \frac{1}{2} N_y W \int_\phi^{\frac{\pi}{2}} f_m(R_b)\cos 2j\theta\, d\theta \qquad \text{for } m = 1,\ldots,M \qquad (A\text{-}33)$$

$$T_{j,m} \;=\; -\frac{1}{2} N_x L \int_0^\phi f_{m\text{-}M}(R_b)\sin 2j\theta\tan\theta\, d\theta$$

$$\qquad +\; \frac{1}{2} N_y W \int_\phi^{\frac{\pi}{2}} f_{m\text{-}M}(R_b)\sin 2j\theta\cot\theta\, d\theta \qquad \text{for } m = M+1,\ldots,2M \qquad (A\text{-}34)$$

These integrals can be evaluated numerically using Simpson's rule. Finally, the vector of unknown displacement field parameters $\{q\}$ in Equation A-17 can be written in the partitioned form

$$\{q\} \;=\; \left\{ \begin{array}{c} \{q_0\} \\ \{q_1\} \\ \vdots \\ \{q_j\} \\ \vdots \\ \{q_N\} \end{array} \right\} \qquad\qquad (A\text{-}35)$$

where $\{q_0\}$ is an M x 1 vector and the remaining partitions are 2M x1 vectors.

Solution of the system of linear algebraic equations represented by Equation A-17 yields the vector of displacement field parameters $\{q\}$. Displacements, strains, and stress resultants at any point in the cutout panel can be calculated by evaluating Equations A-1, A-4, and A-9, respectively.
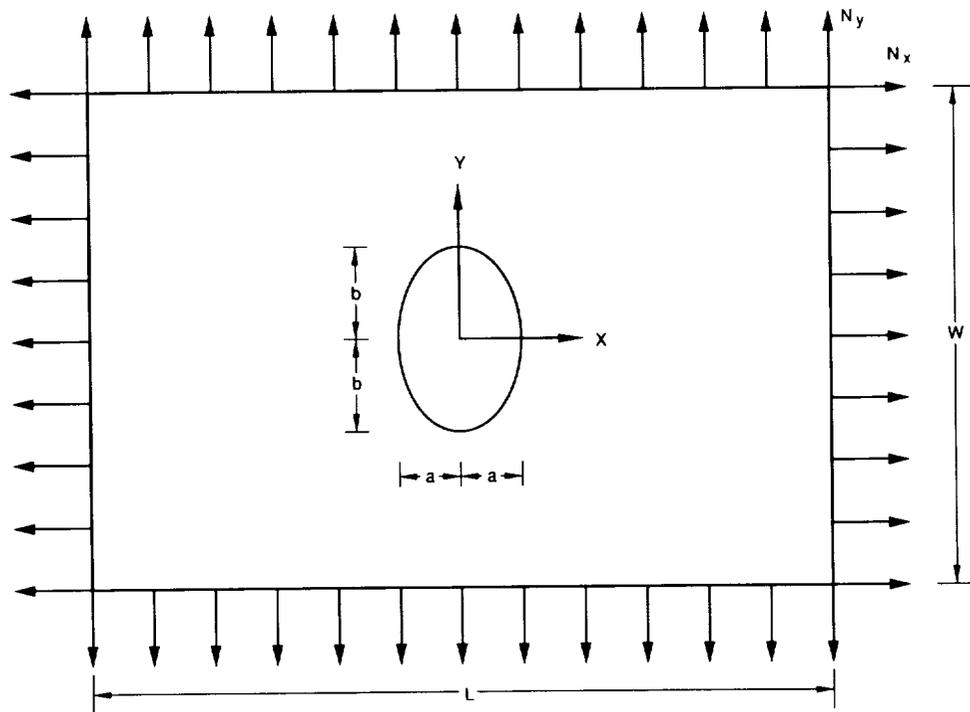
Figure 1. Geometry for cutout analysis methodology.

Section **B – B'**
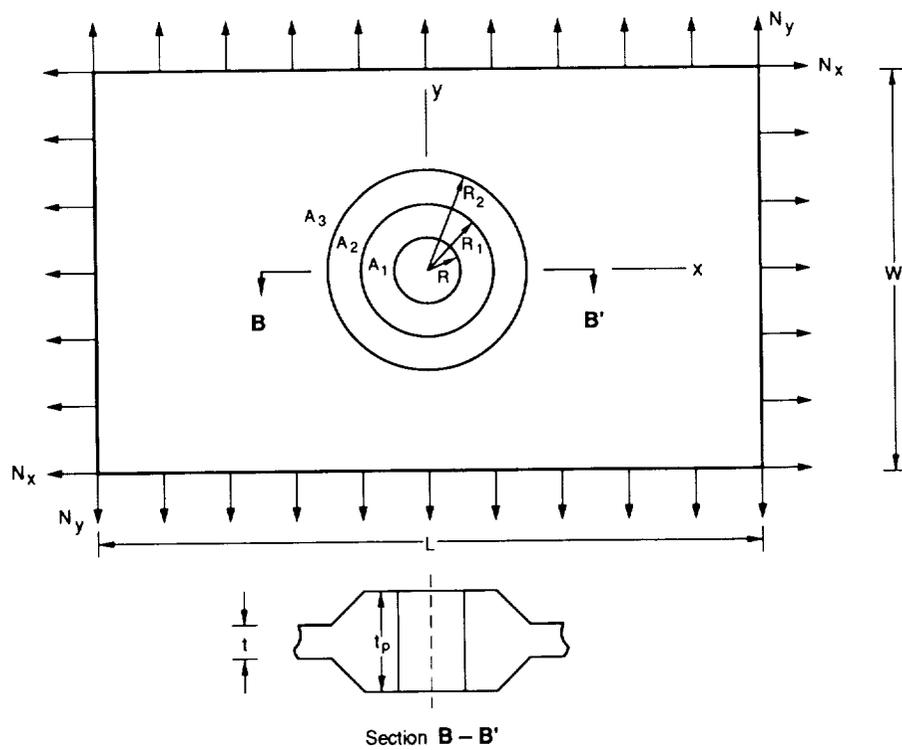
Figure 2. Symmetric integral padup around a circular hole.

916
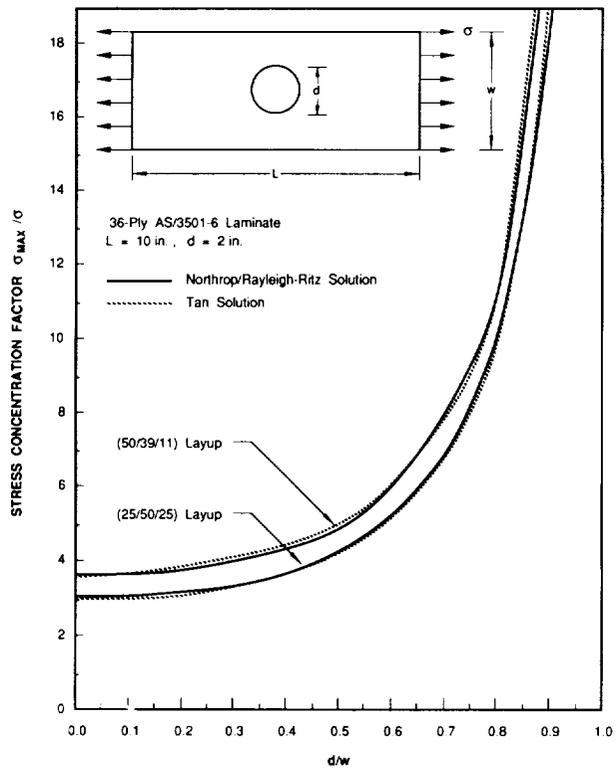
Figure 3. Benchmark results for finite structure circular cutout analysis.
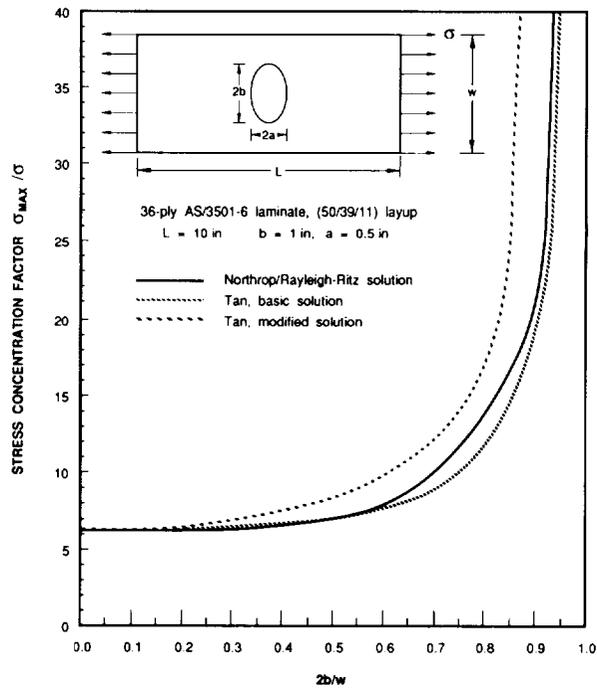
Figure 4. Benchmark results for finite structure elliptical cutout analysis.
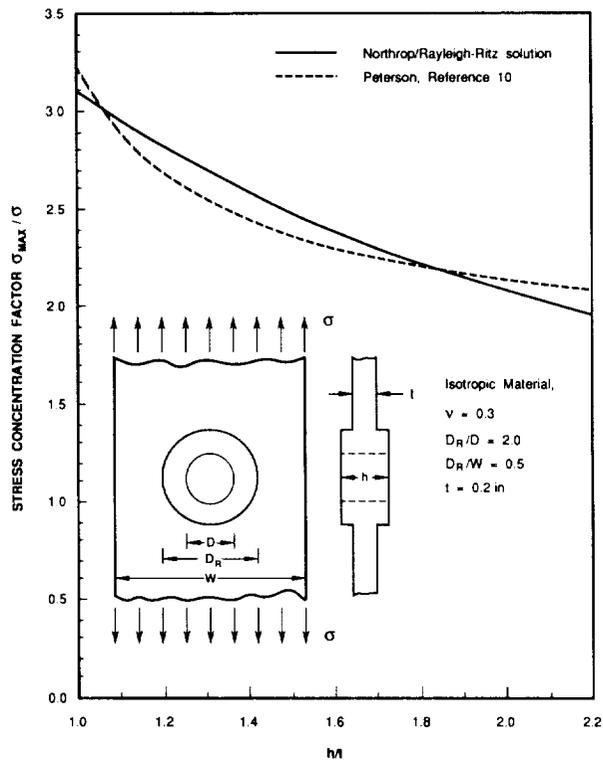
Figure 5. Benchmark results for uniform thickness circular padups.
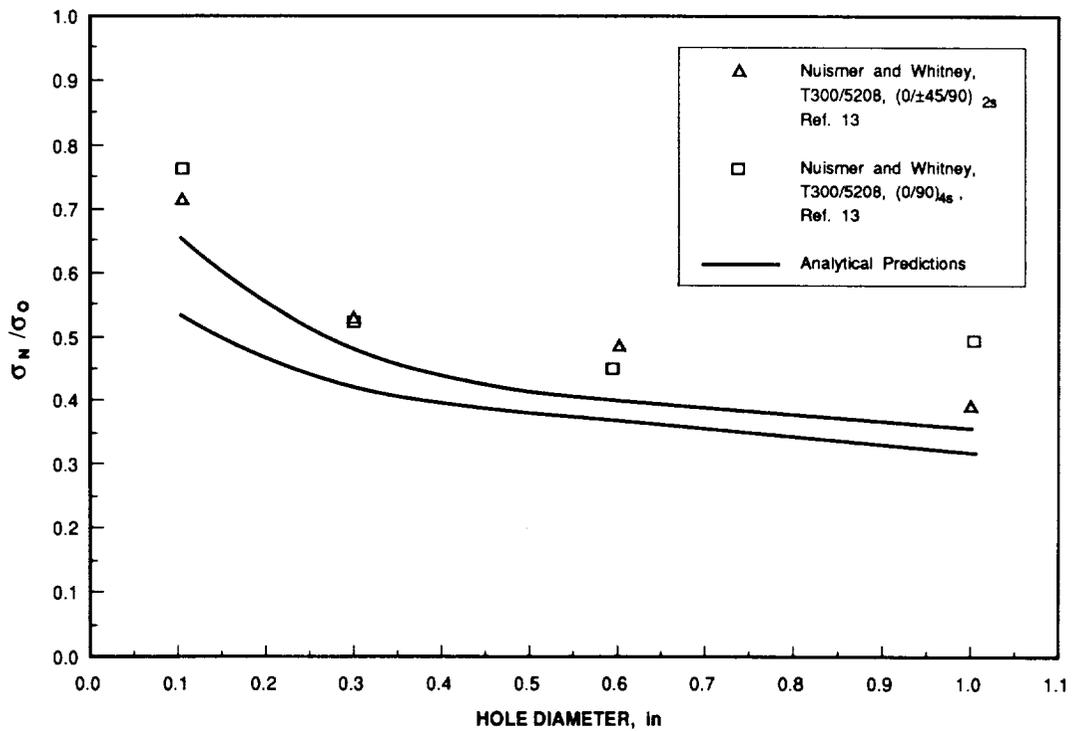
Figure 6. Analytical strength predictions and experimental data for different hole sizes.
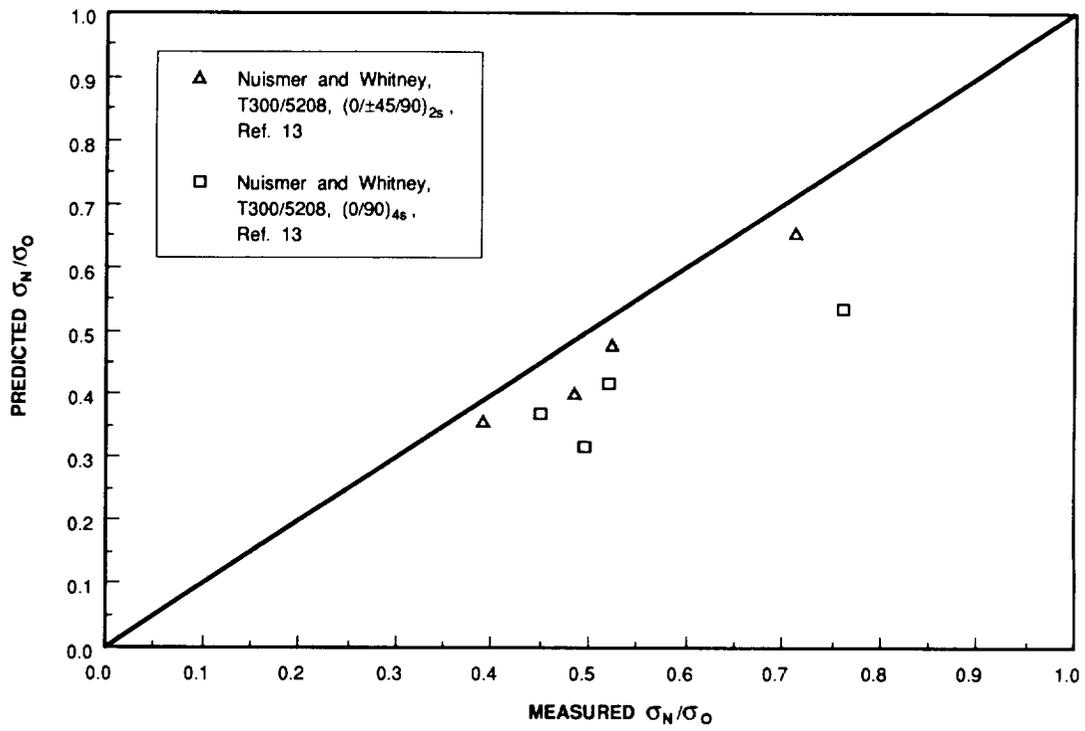
Figure 7. Analytical strength predictions versus experimental data.
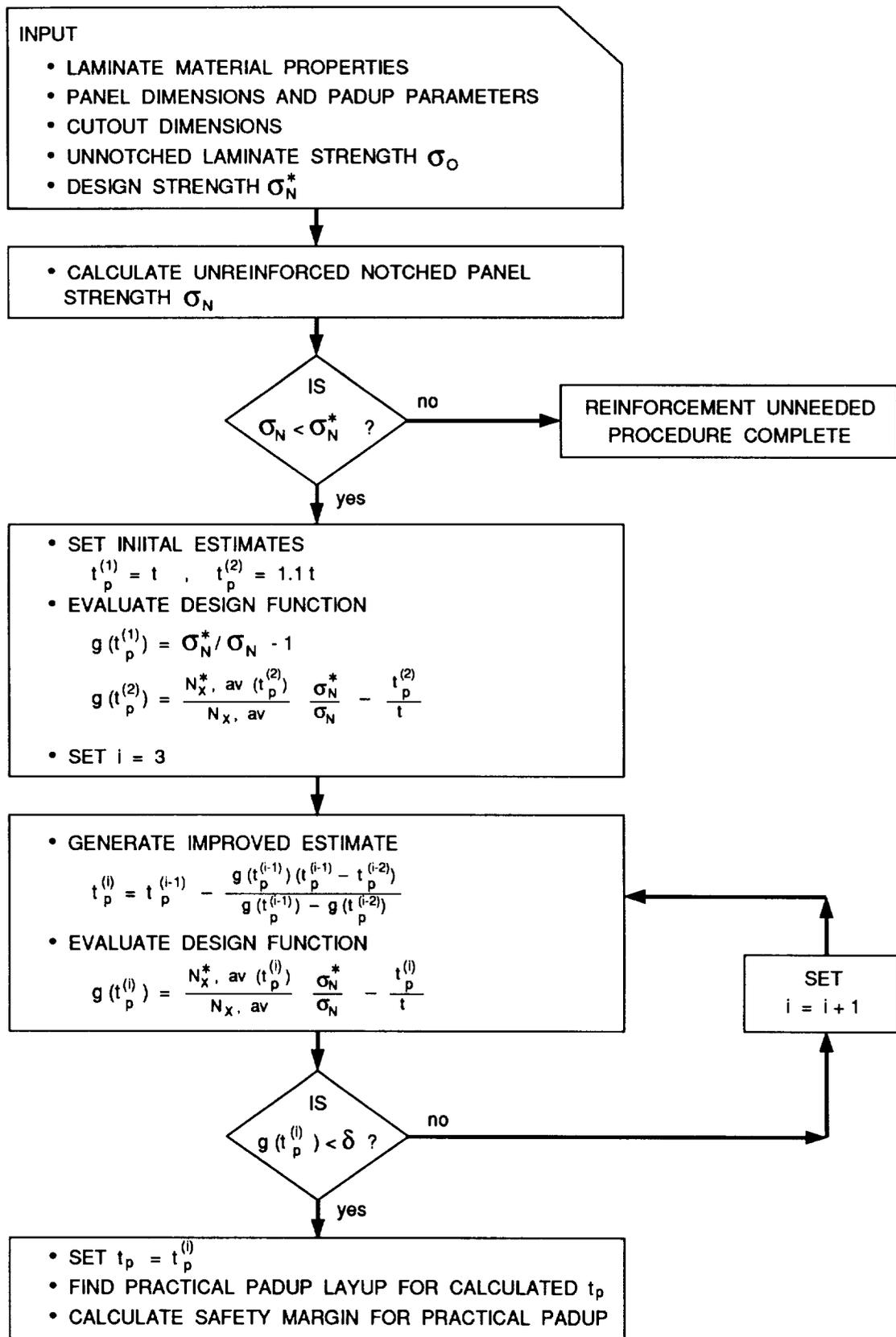
Figure 8. Flowchart for Padup Design Procedure.